Accepted Manuscript

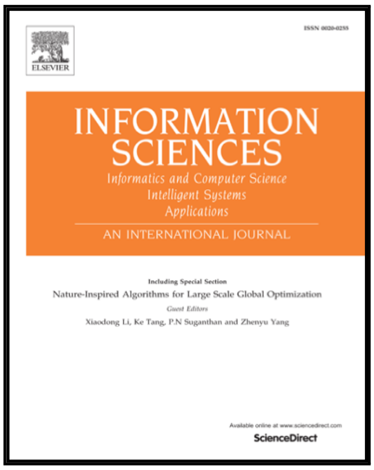

Domain Class Consistency based Transfer Learning for Image Classification Across Domains

Lei Zhang , Jian Yang , David Zhang

PII: S0020-0255(16)31315-9
DOI: 10.1016/j.ins.2017.08.034
Reference: INS 13038

To appear in: *Information Sciences*

Received date: 17 October 2016
Revised date: 30 July 2017
Accepted date: 4 August 2017

Please cite this article as: Lei Zhang , Jian Yang , David Zhang , Domain Class Consistency based Transfer Learning for Image Classification Across Domains, *Information Sciences* (2017), doi: 10.1016/j.ins.2017.08.034

Domain Class Consistency based Transfer Learning for Image Classification Across Domains

Lei Zhang[1,*], Jian Yang[2], and David Zhang[3]

[1]College of Communication Engineering, Chongqing University, Chongqing 400044, China

[2]School of Computer Science and Engineering, Nanjing University of Science and Technology, Nanjing, China

[3]Department of Computing, The Hong Kong Polytechnic University, Hong Kong

*Corresponding author: leizhang@cqu.edu.cn

Abstract

Distribution mismatch between the modeling data and the query data is a known domain adaptation issue in machine learning. To this end, in this paper, we propose a $l_{2,1}$-norm based discriminative robust kernel transfer learning (DKTL) method for high-level recognition tasks. The key idea is to realize robust domain transfer by simultaneously integrating *domain-class-consistency* (DCC) metric based discriminative subspace learning, kernel learning in reproduced kernel Hilbert space, and representation learning between source and target domain. The DCC metric includes two properties: *domain-consistency* used to measure the between-domain distribution discrepancy and *class-consistency* used to measure the within-domain class separability. The essential objective of the proposed transfer learning method is to maximize the DCC metric, which is equivalently to minimize the *domain-class-inconsistency* (DCIC), such that domain distribution mismatch and class inseparability are well formulated and unified simultaneously. The merits of the proposed method include (1) the robust sparse coding selects a few valuable source data with noises (outliers) removed during knowledge transfer, and (2) the proposed DCC metric can pursue more discriminative subspaces of different domains. As a result, the maximum class-separability is also well guaranteed. Extensive experiments on a number of visual datasets demonstrate the superiority of the proposed method over other state-of-the-art domain adaptation and transfer learning methods.

Keywords —Transfer learning; representation learning; subspace learning; kernel learning; domain adaptation

1. Introduction

One basic assumption of machine learning is that the training data and testing data should hold similar probability distribution, i.e. independent identical distribution (*i.i.d*) which shares the same feature subspace. However, in many real applications, machine learning faces with the dilemma of insufficient labeled data. For learning a robust classification model, researchers have to "borrow" more data from other domains for training. One problem of the borrowed data is that the distribution mismatch between *source* domain and *target* domain violates the basic assumption of machine learning. Specifically, domain mismatch often results from a variety of visual cues or abrupt feature changes, such as camera viewpoint, resolution (*e.g.* image sensor from webcam to DSLR), illumination conditions, color correction, poses (*e.g.* faces with different angles), and background, etc. Physically, such distribution mismatch or domain shift is common knowledge in vision problems. With this violation, significant performance degradation is suffered in classification [2]. For example, given a typical object recognition scenario in computer vision, users often recognize a given query object captured by a mobile phone via a well-trained model using the labeled training data from an existing object dataset, such as Caltech 256 [14] or web images. However, these training data may be sampled under different ambient visual cues from the query image. As a result, a failure will be encountered during users' testing process. Some example images of objects from different domains are shown in Fig. 1, which explicitly shows the domain shifts/bias.

In order to deal with such domain distribution mismatch issues, transfer learning and domain adaptation based methods have been emerged [4, 13, 16, 20, 32, 33, 40, 41, 42], which can be generally divided into two categories: classifier-based and feature-based. Specifically, the classifier based methods advocate learning a transfer classifier on the source data, by leveraging a few labeled data from the target domain simultaneously [1, 4, 5, 6, 40, 42]. The "borrowed" target data implies the role of regularization, which can trade-off the decision boundary, such that the learned decision function (*e.g.* SVM) is posed the transfer capability and can be used for classification of domains with bias. The idea of classifier based techniques is straightforward and easy to understand, however, during the decision boundary determination, a number of labeled data are necessary, which may increase the cost of data labeling. Essentially, the classifier based methods attempt to learn a generalized decision function without mining the intrinsic visual drifting mechanism, thus they cannot solve the distribution mismatch fundamentally.

Fig. 1. Examples of object images from 4 sources: Amazon (1st row), DSLR (2nd row), Webcam (3rd row) and Caltech (4th row).

Further, the feature based representation and transformation methods [9, 12, 13, 43, 44] aim at aligning the domain shift by adapting features from the source domain to target domain without training classifiers. Although these methods have been proven to be effective for domain adaptation, two issues still exist. First, for representation based adaptation, the noise and outliers from source data may also be transferred to target data due to overfitting of naïve transformation, which leads to significantly distorted and corrupted data structure. Second, the learned subspace is suboptimal, due to the fact that the subspace and the representation (e.g. global low-rank, local sparse coding etc.) are learned independently, which limits the transfer ability. Third, nonlinear transfer often happens in real application, and cannot be effectively interpreted by using linear reconstruction. Therefore, subspace learning and kernel learning that help most to representation transfer and nonlinear transfer should be conducted and integrated simultaneously.

Additionally, Long, *et al*. [24, 25] proposed class-wise adaptation regularization method (ARTL) which learns an adaptive classifier by jointly optimizing the structural risk and distribution matching between both marginal and conditional distribution for transfer learning. Considering the labeling cost of target domain, unsupervised domain adaptation methods have been proposed [11, 26]. By leveraging the strong learning capability of deep learning, with the convolution neural network (CNN) and maximum mean discrepancy (MMD) criteria, deep transfer learning methods such as residual transfer network (RTN) [27], deep adaptation network (DAN) [28, 29], and joint CNN model [37, 38] have also been proposed. Deep transfer learning depends on pre-trained knowledge network on a larger dataset (*e.g.* ImageNet), so that the transfer performance is greatly improved. In this paper, the proposed method is essentially a shallow transfer learning model, therefore, for comparing with deep transfer models, the CNN based deep features (*e.g.* DeCAF) are exploited in this paper.

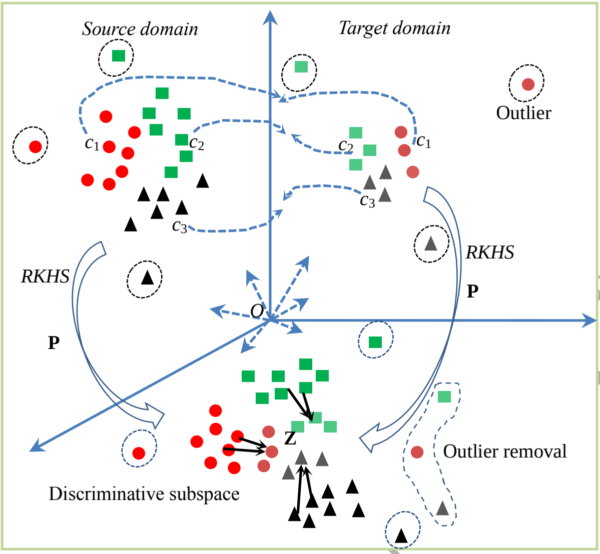

Fig. 2. Schematic diagram of the proposed DKTL method. The data points of 3 classes (*i.e.* c_1, c_2, and c_3) with different marker are included in source domain and target domain. The space distribution disparity and potential outliers per class are clearly shown. Our task is to learn a discriminative subspace projection **P** in RKHS, such that the data points from both domains can lie in a shared subspace where the sparse reconstruction (representation) is implemented for learning such a correspondence **Z** robust to outliers.

As described in Fig.2, in this paper, we propose a novel model which targets at learning a discriminative subspace **P** by using a newly proposed *domain-class-consistency* metric, a reproduced kernel Hilbert space, and a $l_{2,1}$-norm constrained representation. This work is an extension of the IJCNN conference paper [45], by adding more detailed algorithmic deduction and discussion throughout the paper, conducting new experiments on benchmark datasets, introducing parameter sensitive analysis, empirical comparison of computational time, and comparing with more deep transfer learning methods. The proposed method has three merits:

(1) It can learn a discriminative subspace for each domain and guarantee the maximum separability of different classes (*i.e.* c_1, c_2, c_3.) within the same domain. In the model, we formulate to maximize the inter-class distance within the same domain, such that the inter-class difference within a domain can cover the between-domain discrepancy. In this way, the inter-class difference can be enhanced and the impact of distribution mismatch is thus reduced, such that the proposed method is not sensitive to domain bias. This is

motivated by the fact that in face recognition, the difference between two images of the same person captured under different illumination condition may be larger than that of two persons captured under the same condition.

(2) By imposing $l_{2,1}$-norm constraint on the transfer representation coefficient **Z** between source and target data points, only a few valuable source data points are utilized, such that the outliers in the source domain can be well removed without incorrectly transferring to the target domain. Therefore, the proposed method is not sensitive to noises or implicit outliers during transferring. Additionally, with the $l_{2,1}$-norm constraint on **Z**, the closed-form solution can be obtained with a higher computational efficiency than l_1-norm sparse constraint or low-rank constraint.

(3) Due to the fact that nonlinear domain shift may often be encountered in complex vision applications, the kernel learning idea using an implicit nonlinear mapping function for approximated linear separability in the reproduced kernel Hilbert space (*RKHS*) is naturally motivated. With the above description, discriminative subspace learning, representation learning and kernel learning are formulated in the proposed method. For convenience, we call our method discriminative kernel transfer learning (DKTL).

The rest of this paper is organized as follows. Section 2 summarizes the related work in transfer learning and domain adaptation. The proposed model and optimization algorithms are presented in Section 3. The experiments on a number of datasets for transfer learning tasks and discussions are conducted in Section 4. The parameter sensitivity and computational time analysis are provided in Section 5. Finally, a concluding remark of the present work is given.

2. Related Work

In recent years, a number of transfer learning and domain adaptation methods have been proposed, which are summarized as two categories: classifier adaptation based methods and feature adaptation based methods.

For the former, Yang *et al.* [40] proposed an adaptive support vector machine (ASVM), which aims at learning the perturbation term for adapting the source classifier to the target classifier. Collobert *et al.* [1] proposed a transductive SVM (T-SVM), which utilized the labeled and unlabeled samples simultaneously. Duan *et al.* [5] proposed a domain adaptation machine (DAM) method which integrates SVM for classifier adaptation. With the SVM based classifier adaptation idea, they also proposed an adaptive multiple kernel learning method (AMKL) [6] and a domain transfer MKL (DTMKL or DTSVM) [4] methods, by integrating multiple kernels for improving the robustness and classification accuracy. Zhang *et al.* proposed a domain adaptation ELM method for classifier adaptation [42], and also proposed a robust extreme domain adaptation (EDA) [46] method by using Laplacian graph regularization for local structure preservation and achieve state-of-the-art results. Zheng *et al*. [47] proposed a hetero-manifold regularization method (HMR) for cross-modal hashing and achieves good results on cross-modal tasks. Shekhar *et al.* [36] proposed a domain adaptive dictionary learning method (SDDL) for representation classifier adaptation. Zhu and Shao [48] also proposed a cross-domain dictionary learning method (WSCDDL) for weakly-supervised transfer learning based on representation classifier adaptation. Based on the cross-domain dictionary learning, Zhu *et al*. [49] proposed a boosted cross-domain categorization (BCDC) method and a more robust cross-domain classifier was contributed.

For the latter, Gopalan *et al.* [13] proposed a SGF method for unsupervised domain adaptation via low dimensional subspace transfer. The idea behind SGF is that it samples a group of subspaces along the geodesic between source and target data, and project the source data into the subspaces for discriminative classifier learning. Gong *et al.* [12] proposed an unsupervised domain adaptation method (GFK) for visual domain adaptation, in which geodesic flow kernel is used to model the domain shift by integrating an infinite number of subspaces, where the geometric and statistical properties are characterized. Zhang *et al.* [43] proposed a latent sparse domain transfer (LSDT) method by using sparse subspace reconstruction for visual adaptation. Fernando *et al*. [9] proposed principal component subspace alignment (SA) for subspace transfer. More recently, low rank representation (LRR) based domain adaptation is proposed. Two representative work can be referred as [18, 34], in which LRR based method are proposed for aligning the domain shifts. As referred by Liu *et al*. [22, 23], LRR can get the block diagonal solution and performs perfectly for subspace segmentation when the subspaces are independent and the data sampling is sufficient. However, when handling disjoint subspace problems and insufficient data, LRR will not work well. Therefore, LRR based domain adaptation capability will be restricted because of such strong independent subspace assumption. An excellent survey on transfer learning for visual categorization by Shao, *et al.* can be referred to as [35], which has well explored the existing methods.

As indicated by the sparse subspace clustering (SSC) [7, 8], which were proposed for clustering data points that lie in a union of multiple low-dimensional subspaces or near the intersections of subspaces, the reconstruction error $\|\mathbf{X}-\mathbf{XZ}\|_F$ is minimized by imposing sparsity constraint on **Z**. Therefore, in transfer learning tasks, the cross-domain reconstruction error $\|\mathbf{X}_T-\mathbf{X}_S\mathbf{Z}\|_F$ is expected to be minimized for adapting source data to target data lying in different subspaces. However, this reconstruction error minimization problem only guarantees the data consistency, but missing the domain transfer property. That is, there is no knowledge adaptation based on such naïve least square. Therefore, we propose to achieve the minimization in some latent subspace **P**, *i.e.* $\|\mathbf{PX}_T-\mathbf{PX}_S\mathbf{Z}\|_F$. Also, to guarantee the inter-class separability in the subspace, discriminative subspace with domain-class-consistency (*i.e.* DCC) can be simultaneously learned.

3. Proposed Discriminative Kernel Transfer Learning

3.1. Notations

In this paper, the source and target domain are defined by subscript "*S*" and "*T*". The training set of source and target domain is defined as $\mathbf{X}_S \in \Re^{D\times N_S}$ and $\mathbf{X}_T \in \Re^{D\times N_T}$, where D denotes the dimension of data, N_S and N_T denote the number of samples of source and target domain, respectively. Let $\mathbf{P}\in\Re^{D\times d}$ $(d\le D)$ represent the discriminative basis transformation that maps the original data space of the source and target data into a d dimensional subspace. The reconstruction coefficient matrix is denoted as **Z**, and **I** denotes the identity matrix. $\|\cdot\|_p$, $\|\cdot\|_{q,p}$ and $\|\cdot\|_F$ denote l_p-norm, $l_{q,p}$-norm and Frobenius norm, respectively. The superscript $^{\mathrm{T}}$ denotes the transpose operator, and $Tr(\cdot)$ denotes the trace operator of a matrix.

3.2. Problem Formulation

As illustrated in Fig. 2, we tend to learn a representation matrix **Z** for reconstructing the target data $\mathbf{X}_T$ by using the source data $\mathbf{X}_S$ in their discriminative subspace projected by a group of basis, *i.e.* **P**. Therefore, the general framework of the proposed DKTL can be formulated as

$$\begin{aligned}&\min_{\mathbf{P},\mathbf{Z}} E(\mathbf{X}_S,\mathbf{X}_T,\mathbf{P},\mathbf{Z})+\lambda\cdot\Omega(\mathbf{P})+\tau\cdot R(\mathbf{Z})\\ &s.t.\ \mathbf{P}^{\mathrm{T}}\mathbf{P}=\mathbf{I},\ \lambda,\tau>0\end{aligned} \tag{1}$$

where $E(\cdot)$ represents the *domain-inconsistency* term (i.e. cross domain representation or reconstruction error), $\Omega(\cdot)$ denotes the *class-inconsistency* term (i.e. discriminative regularizer) among multiple domains,

$R(\cdot)$ represents the model regularization term of the representation coefficients with robust outlier removal, λ and τ represent the positive regularization parameters. The constraint condition $\mathbf{P}^{\mathrm{T}}\mathbf{P} = \mathbf{I}$ guarantees the normalized orthogonal subspace of $\mathbf{P}$.

From the optimization problem (1), it is obvious that by jointly minimizing the *domain-inconsistency* and *class-inconsistency*, *i.e.* DCIC, the domain-class-consistency (DCC) can be strengthened such that the proposed DKTL not only realizes the domain transfer (i.e. domain consistency), but also enhances the class separability (i.e. class consistency). Therefore, the proposed model is more robust for classification-oriented transfer learning tasks. Note that maximization of the domain-class-consistency (DCC) is equivalent to minimize the domain-class-inconsistency (DCIC), but for easier formulation, a DCIC minimization problem is solved in this paper.

Suppose that $\mathbf{P}$ can be represented by a linear combination of the transformed training samples $\varphi(\mathbf{X}) = [\varphi(\mathbf{X}_S), \varphi(\mathbf{X}_T)]$, which can be written as

$$\mathbf{P} = \varphi(\mathbf{X})\mathbf{\Phi} \tag{2}$$

where $\mathbf{\Phi} \in \Re^{N\times d}$ denotes the linear combination coefficients, $\varphi(\cdot)$ is some implicit linear/nonlinear mapping function imposed on the raw data, and N=N_S+N_T.

Specifically, by substituting Eq.(2) and the mapping function $\varphi(\cdot)$ into the first term of Eq.(1), then the reconstruction error expression $E(\cdot)$ can be formulated as follows

$$\begin{aligned} E(\mathbf{X}_S, \mathbf{X}_T, \mathbf{P}, \mathbf{Z}) &= \left\| \mathbf{P}^{\mathrm{T}}\varphi(\mathbf{X}_T) - \mathbf{P}^{\mathrm{T}}\varphi(\mathbf{X}_S)\mathbf{Z} \right\|_{\mathrm{F}}^2 \\ &= \left\| \mathbf{\Phi}^{\mathrm{T}}\varphi(\mathbf{X})^{\mathrm{T}}\varphi(\mathbf{X}_T) - \mathbf{\Phi}^{\mathrm{T}}\varphi(\mathbf{X})^{\mathrm{T}}\varphi(\mathbf{X}_S)\mathbf{Z} \right\|_{\mathrm{F}}^2 \end{aligned} \tag{3}$$

where $\mathbf{Z} \in \Re^{N_S \times N_T}$ denotes the cross domain representation coefficient matrix. Obviously, the smaller the representation error $E(\cdot)$ is, the better the domain consistency is. Therefore, by minimizing the reconstruction error in the latent subspace, the domain consistency can be enhanced.

The second term $\Omega(\mathbf{P})$ in Eq.(1) pursuits a discriminative subspace where the domain-class-inconsistency (DCIC) is minimized. As the name suggests, the DCIC includes two parts: domain inconsistency (minimized) and class inconsistency (maximized). Therefore, the DCIC term can be formulated as

$$\begin{aligned}\Omega(\mathbf{P}) &= \sum_{c=1}^{C}\left\|\mathbf{P}^{\mathrm{T}}\varphi\left(\boldsymbol{\mu}_S^c\right)-\mathbf{P}^{\mathrm{T}}\varphi\left(\boldsymbol{\mu}_T^c\right)\right\|_2^2-\sum_{t\in\{S,T\}}\sum_{c,k=1,c\neq k}^{C}\left\|\mathbf{P}^{\mathrm{T}}\varphi\left(\boldsymbol{\mu}_t^c\right)-\mathbf{P}^{\mathrm{T}}\varphi\left(\boldsymbol{\mu}_t^k\right)\right\|_2^2 \\ &= \sum_{c=1}^{C}\left\|\boldsymbol{\Phi}^{\mathrm{T}}\varphi(\mathbf{X})^{\mathrm{T}}\varphi\left(\boldsymbol{\mu}_S^c\right)-\boldsymbol{\Phi}^{\mathrm{T}}\varphi(\mathbf{X})^{\mathrm{T}}\varphi\left(\boldsymbol{\mu}_T^c\right)\right\|_2^2-\sum_{t\in\{S,T\}}\sum_{c,k=1,c\neq k}^{C}\left\|\boldsymbol{\Phi}^{\mathrm{T}}\varphi(\mathbf{X})^{\mathrm{T}}\varphi\left(\boldsymbol{\mu}_t^c\right)-\boldsymbol{\Phi}^{\mathrm{T}}\varphi(\mathbf{X})^{\mathrm{T}}\varphi\left(\boldsymbol{\mu}_t^k\right)\right\|_2^2\end{aligned} \tag{4}$$

where $\varphi\left(\boldsymbol{\mu}_S^c\right)=\frac{1}{N_S^c}\sum_{i=1}^{N_S^c}\varphi\left(\mathbf{X}_{S,i}^c\right)$ and $\varphi\left(\boldsymbol{\mu}_T^c\right)=\frac{1}{N_T^c}\sum_{i=1}^{N_T^c}\varphi\left(\mathbf{X}_{T,i}^c\right)$ represent the centroid of class c of source and target training data after $\varphi(\cdot)$ mapping, respectively. The first term in Eq.(4) denotes the between-domain intra-class inconsistency (i.e. the same class in different domain) that expects to be minimized and the second term in Eq.(4) denotes the within-domain inter-class consistency (i.e. different class in the same domain) that expects to be maximized. Note that a very few labeled target data should be used during the computation of Eq.(4) in the proposed method, that is, DKTL is not unsupervised. However, it is not difficult to obtain an unsupervised variant by only considering the labeled source data. For example, for the target domain data, the centroid of the unlabeled target data can be computed for measuring inter-domain discrepancy. By minimizing the difference between the intra-class inconsistency and the inter-class consistency, the discriminative subspace can be well achieved. Consequently, the generalized domain-class-consistency can be well shown, and the discriminative learning can effectively improve the classification-oriented domain transfer performance.

The third term $R(\mathbf{Z})$ in Eq.(1) is a robust sparse constraint on the transfer coefficients $\mathbf{Z}$ for regularization. Generally, it can be formulated as follows

$$R(\mathbf{Z})=\|\mathbf{Z}\|_{q,p} \tag{5}$$

where $\|\cdot\|_{q,p}$ represents $l_{q,p}$-norm. Given a matrix $\mathbf{Q}\in\Re^{m\times n}$, then there is

$$\|\mathbf{Q}\|_{q,p}=\left(\sum_{i=1}^{m}\left(\sum_{j=1}^{n}\left|Q_{i,j}\right|^q\right)^{p/q}\right)^{1/p} \tag{6}$$

As can be seen from Eq.(6), a common Frobenius norm is achieved when p=q=2. Intrinsically, different approaches may be induced by selecting different p and q-values. Generally, for sparsity pursuit, $q\geq2$ and $0\leq p\leq2$ may be required. If p=0, the induced l_0-norm sub-problem is not convex and therefore p=1 is used in this paper for sparse approximation. Since q is used to measure the row vector norm, q=2 is set based on the consideration that larger q does not improve the results [17]. Therefore, the Eq.(5) can be formulated by $l_{2,1}$-norm as $R(\mathbf{Z}) = \|\mathbf{Z}\|_{2,1}$ for better sparsity and robustness to outliers. The property of $l_{2,1}$-norm guarantees that the outliers in source data can be automatically avoided during representation transfer. In this way, the implicit outliers in source domain may not be transferred to target domain via $l_{2,1}$-norm minimization, such that the generalization is achieved.

Finally, by substituting Eqs.(3), (4) and (5) into Eq.(1), the proposed DKTL model can be formulated as follows

$$\begin{aligned}&\min_{\mathbf{\Phi},\mathbf{Z}}\left\|\mathbf{\Phi}^{\mathrm{T}}\varphi(\mathbf{X})^{\mathrm{T}}\varphi(\mathbf{X}_T)-\mathbf{\Phi}^{\mathrm{T}}\varphi(\mathbf{X})^{\mathrm{T}}\varphi(\mathbf{X}_S)\mathbf{Z}\right\|_{\mathrm{F}}^2+\lambda\cdot\left(\sum_{c=1}^{C}\left\|\mathbf{\Phi}^{\mathrm{T}}\varphi(\mathbf{X})^{\mathrm{T}}\varphi(\boldsymbol{\mu}_S^c)-\mathbf{\Phi}^{\mathrm{T}}\varphi(\mathbf{X})^{\mathrm{T}}\varphi(\boldsymbol{\mu}_T^c)\right\|_2^2-\right.\\&\left.\sum_{t\in\{S,T\}}\sum_{c,k=1,c\neq k}^{C}\left\|\mathbf{\Phi}^{\mathrm{T}}\varphi(\mathbf{X})^{\mathrm{T}}\varphi(\boldsymbol{\mu}_t^c)-\mathbf{\Phi}^{\mathrm{T}}\varphi(\mathbf{X})^{\mathrm{T}}\varphi(\boldsymbol{\mu}_t^k)\right\|_2^2\right)+\tau\cdot\|\mathbf{Z}\|_{2,1}\\&s.t.\ \mathbf{\Phi}^{\mathrm{T}}\varphi(\mathbf{X})^{\mathrm{T}}\varphi(\mathbf{X})\mathbf{\Phi}=\mathbf{I},\ \lambda,\tau>0\end{aligned}\tag{7}$$

According to the Mercer kernel theorem and inner product, we define the following kernel matrices,

$$\mathbf{K}=\varphi(\mathbf{X})^{\mathrm{T}}\varphi(\mathbf{X})=\kappa(\mathbf{X},\mathbf{X})$$

$$\mathbf{K}_T=\varphi(\mathbf{X})^{\mathrm{T}}\varphi(\mathbf{X}_T)=\kappa(\mathbf{X},\mathbf{X}_T)$$

$$\mathbf{K}_S=\varphi(\mathbf{X})^{\mathrm{T}}\varphi(\mathbf{X}_S)=\kappa(\mathbf{X},\mathbf{X}_S)$$

$$\mathbf{K}_{\mu,S}^c=\varphi(\mathbf{X})^{\mathrm{T}}\varphi(\boldsymbol{\mu}_S^c)=\kappa(\mathbf{X},\boldsymbol{\mu}_S^c)$$

$$\mathbf{K}_{\mu,T}^c=\varphi(\mathbf{X})^{\mathrm{T}}\varphi(\boldsymbol{\mu}_T^c)=\kappa(\mathbf{X},\boldsymbol{\mu}_T^c)$$

Then the proposed DKTL model (7) can be reformulated as

$$\begin{aligned}&\min_{\mathbf{\Phi},\mathbf{Z}}\left\|\mathbf{\Phi}^{\mathrm{T}}\mathbf{K}_T-\mathbf{\Phi}^{\mathrm{T}}\mathbf{K}_S\mathbf{Z}\right\|_{\mathrm{F}}^2+\lambda\cdot\left(\frac{1}{C}\sum_{c=1}^{C}\left\|\mathbf{\Phi}^{\mathrm{T}}\mathbf{K}_{\mu,S}^c-\mathbf{\Phi}^{\mathrm{T}}\mathbf{K}_{\mu,T}^c\right\|_2^2-\right.\\&\qquad\left.\frac{2}{C(C-1)}\sum_{t\in\{S,T\}}\alpha_t\sum_{c,k=1,c\neq k}^{C}\left\|\mathbf{\Phi}^{\mathrm{T}}\mathbf{K}_{\mu,t}^c-\mathbf{\Phi}^{\mathrm{T}}\mathbf{K}_{\mu,t}^k\right\|_2^2\right)+\tau\cdot\|\mathbf{Z}\|_{2,1}\\&s.t.\ \mathbf{\Phi}^{\mathrm{T}}\mathbf{K}\mathbf{\Phi}=\mathbf{I},\ \alpha_S+\alpha_T=1,\lambda,\tau,\alpha_S,\alpha_T>0\end{aligned}\tag{8}$$

where the coefficient α_S and α_T represent the weights of source and target domain, which are used to weight the within-domain inter-class difference and improve class-consistency (e.g. if source domain has larger inter-class discrepancy than target domain, and therefore α_S should be slightly larger than α_T). λ and τ represent the regularization parameters for DCIC term and reconstruction matrix $\mathbf{Z}$, respectively, which are used to trade-off the domain transfer performance. $\mathbf{K}$, $\mathbf{K}_S$, and $\mathbf{K}_T$ denote the kernel Gram matrix of the combined data, source data and target data, respectively. $\mathbf{K}_{\mu,S}^c$ and $\mathbf{K}_{\mu,T}^c$ denote the kernel mean vectors with respect to class c of source data and target data, respectively. $\kappa(\cdot)$ represents the kernel function. From Equation (8), it is clear that the proposed transfer learning model is transformed into a kernel reconstruction framework in RKHS space. Generally, the effect of kernel is to reproduce a rich embedding space where the distribution matching (i.e. domain transfer) can be easily implemented. Although different kernel functions such as polynomial kernel, perceptron kernel (i.e. sigmoid), etc. can be used, Gaussian kernel can reproduce richer embedding space for transferring.

Therefore, in this paper, the Gaussian kernel function is used, and it can be represented with kernel parameter σ by

$$\kappa(\mathbf{x},\mathbf{y}) = \exp\left(-\|\mathbf{x}-\mathbf{y}\|_2^2 \big/ 2\sigma^2\right) \tag{9}$$

From Eq.(8), it is clear that this is a non-convex optimization problem with respect to two variables $\mathbf{\Phi}$ and $\mathbf{Z}$. However, it becomes a convex problem with respect to one variable by fixing the other one. Therefore, a common variable alternating optimization algorithm is proposed for near-optimal solutions. The specific solving process is presented as follows.

3.3. Optimization

The optimization of DKTL model (8) is presented in this section. From Eq.(8), there are two variables $\mathbf{\Phi}$ and $\mathbf{Z}$ in the model. When fix one of them, the model is convex with respect to the other one. Therefore, a variable alternating optimization algorithm is proposed for solving the minimization problem.

✧ **Update Φ:**

By fixing the variable $\mathbf{Z}$, the problem shown in Eq.(8) with respect to $\mathbf{\Phi}$ then becomes

$$\min_{\mathbf{\Phi}} \left\| \mathbf{\Phi}^{\mathrm{T}} \mathbf{K}_T - \mathbf{\Phi}^{\mathrm{T}} \mathbf{K}_S \mathbf{Z} \right\|_{\mathrm{F}}^2 + \lambda \cdot \left(\frac{1}{C} \sum_{c=1}^{C} \left\| \mathbf{\Phi}^{\mathrm{T}} \mathbf{K}_{\mu,S}^{c} - \mathbf{\Phi}^{\mathrm{T}} \mathbf{K}_{\mu,T}^{c} \right\|_2^2 - \frac{2}{C(C-1)} \sum_{t \in \{S,T\}} \alpha_t \sum_{c,k=1,c \neq k}^{C} \left\| \mathbf{\Phi}^{\mathrm{T}} \mathbf{K}_{\mu,t}^{c} - \mathbf{\Phi}^{\mathrm{T}} \mathbf{K}_{\mu,t}^{k} \right\|_2^2 \right)$$
$$s.t.\ \mathbf{\Phi}^{\mathrm{T}} \mathbf{K} \mathbf{\Phi} = \mathbf{I},\ \alpha_S + \alpha_T = 1, \lambda, \alpha_S, \alpha_T > 0 \tag{10}$$

The problem in Eq.(10) can be further written as the following shape

$$\min_{\mathbf{\Phi}} Tr\left(\mathbf{\Phi}^{\mathrm{T}} \mathbf{A} \mathbf{\Phi}\right) \quad s.t.\ \mathbf{\Phi}^{\mathrm{T}} \mathbf{K} \mathbf{\Phi} = \mathbf{I} \tag{11}$$

where $\mathbf{A}$ can be represented as

$$\mathbf{A} = \mathbf{A}_1 + \lambda \cdot \mathbf{A}_2 - \lambda \cdot \mathbf{A}_3 \tag{12}$$

The matrix $\mathbf{A}_1$, $\mathbf{A}_2$ and $\mathbf{A}_3$ in Eq.(12) are computed as

$$\mathbf{A}_1 = \left(\mathbf{K}_T - \mathbf{K}_S \mathbf{Z}\right)\left(\mathbf{K}_T - \mathbf{K}_S \mathbf{Z}\right)^{\mathrm{T}} \tag{13}$$

$$\mathbf{A}_2 = \frac{1}{C} \sum_{c=1}^{C} \left(\mathbf{K}_{\mu,S}^{c} - \mathbf{K}_{\mu,T}^{c}\right)\left(\mathbf{K}_{\mu,S}^{c} - \mathbf{K}_{\mu,T}^{c}\right)^{\mathrm{T}} \tag{14}$$

$$\mathbf{A}_3 = \frac{2}{C(C-1)} \sum_{t \in \{S,T\}} \alpha_t \sum_{c,k=1,c \neq k}^{C} \left(\mathbf{K}_{\mu,t}^{c} - \mathbf{K}_{\mu,t}^{k}\right)\left(\mathbf{K}_{\mu,t}^{c} - \mathbf{K}_{\mu,t}^{k}\right)^{\mathrm{T}} \tag{15}$$

The derivation of Eq.(11) from Eq.(10) is presented in Appendix A, in which the Eq.(12)~Eq.(15) can be derived.

From the minimization model (11), we can see that the Eigen-decomposition can be derived by constructing Lagrange multiplier based objective function. In detail, the optimization of Eq.(11) is shown in Appendix B, from which the optimal solution $\mathbf{\Phi}$ in Eq.(11) can be spanned by the first l eigenvectors with respect to the first l smallest eigenvalues of the matrix $\mathbf{K}^{-1}\mathbf{A}$. Note that in computing $\mathbf{A}_1$, the initialized $\mathbf{Z}$ is required. Therefore, we initialize $\mathbf{Z} = \mathbf{K}_S^{\mathrm{T}} \mathbf{K}_T$ as a warm start.

For easy following, the formularized solving process of $\mathbf{\Phi}$ is summarized in Algorithm 1.

Algorithm 1. Solving $\mathbf{\Phi}$
Input: $\mathbf{K}_S$, $\mathbf{K}_T$, $\mathbf{K}^c_{\mu,S}$, $\mathbf{K}^c_{\mu,T}$, λ, d;
Procedure:
1. Initialize $\mathbf{Z} = \mathbf{K}_S^{\mathrm{T}} \mathbf{K}_T$;
2. Compute $\mathbf{A}_1$, $\mathbf{A}_2$ and $\mathbf{A}_3$ using Eqs.(13), (14), (15), respectively;
3. Compute $\mathbf{A}$ using Eq.(12);
4. Perform Eigen-value decomposition of $\mathbf{K}^{-1}\mathbf{A} = \mathbf{U}\Sigma\mathbf{U}^{\mathrm{T}}$;
5. Get $\mathbf{\Phi} = \mathbf{U}(:,\upsilon)$, where υ is the index of the d smallest Eigen-values;
Output: $\mathbf{\Phi}$

✧ **Update Z:**

By fixing $\mathbf{\Phi}$, the problem in Eq.(8) is transformed into the following problem

$$\min_{\mathbf{Z}} \left\| \mathbf{\Phi}^{\mathrm{T}} \mathbf{K}_T - \mathbf{\Phi}^{\mathrm{T}} \mathbf{K}_S \mathbf{Z} \right\|_{\mathrm{F}}^2 + \tau \cdot \|\mathbf{Z}\|_{2,1} \tag{16}$$

The second term in Eq.(16) can be written as [31].

$$\|\mathbf{Z}\|_{2,1} = Tr\left(\mathbf{Z}^{\mathrm{T}} \mathbf{\Theta} \mathbf{Z}\right) \tag{17}$$

where $\mathbf{\Theta} \in \Re^{N_S \times N_S}$ is a diagonal matrix, whose the i-th diagonal element is calculated as

$$\Theta_{ii} = \frac{1}{2\|\mathbf{Z}_i\|_2} \tag{18}$$

where $\mathbf{Z}_i$ represents the i-th row of matrix $\mathbf{Z}$.

By substituting Eq.(17) into Eq.(16), we have

$$\min_{\mathbf{Z}} \left\| \mathbf{\Phi}^{\mathrm{T}} \mathbf{K}_T - \mathbf{\Phi}^{\mathrm{T}} \mathbf{K}_S \mathbf{Z} \right\|_{\mathrm{F}}^2 + \tau \cdot Tr\left(\mathbf{Z}^{\mathrm{T}} \mathbf{\Theta} \mathbf{Z}\right) \tag{19}$$

As can be seen from model (19), it is differentiable with respect to $\mathbf{Z}$. Let its derivative be 0, we have

$$\left(\mathbf{K}_S^{\mathrm{T}} \mathbf{\Phi} \mathbf{\Phi}^{\mathrm{T}} \mathbf{K}_S + \tau \cdot \mathbf{\Theta}\right) \cdot \mathbf{Z} = \mathbf{K}_S^{\mathrm{T}} \mathbf{\Phi} \mathbf{\Phi}^{\mathrm{T}} \mathbf{K}_T \tag{20}$$

Then, the closed-form solution of **Z** can be expressed as

$$\mathbf{Z}=\left(\mathbf{K}_S^{\mathrm{T}}\mathbf{\Phi}\mathbf{\Phi}^{\mathrm{T}}\mathbf{K}_S+\tau\cdot\mathbf{\Theta}\right)^{-1}\mathbf{K}_S^{\mathrm{T}}\mathbf{\Phi}\mathbf{\Phi}^{\mathrm{T}}\mathbf{K}_T \tag{21}$$

For easy following, the optimization of **Z** is summarized in Algorithm 2.

Although the closed-form solution of **Z** can be achieved, in computing $\mathbf{\Theta}$, the initialized **Z** is required. Therefore, for achieving the optimal solutions $\mathbf{Z}^*$ and $\mathbf{\Phi}^*$ via variable alternating optimization method, several iterations can guarantee the convergence.

Algorithm 2. Solving **Z**

Input: $\mathbf{K}_S$, $\mathbf{K}_T$, $\mathbf{\Phi}$, τ;

Procedure:

1. Initialize $\mathbf{Z}=\mathbf{K}_S^{\mathrm{T}}\mathbf{K}_T$;
2. Compute $\mathbf{\Theta}$ using Eq.(18);
3. Compute **Z** using Eq.(21);

Output: **Z**;

By recalling the optimization of **Φ** in Algorithm 1 and the optimization of **Z** in Algorithm 2, the whole optimization process of the proposed DKTL model shown in Eq.(8) can be summarized in Algorithm 3.

Algorithm 3. Proposed DKTL

Input: $\mathbf{K}_S$, $\mathbf{K}_T$, $\mathbf{K}_{\mu,S}^c$, $\mathbf{K}_{\mu,T}^c$, λ, τ, d, $T_{\max}$;

1. Initialize $\mathbf{Z}=\mathbf{K}_S^{\mathrm{T}}\mathbf{K}_T$ and t=1;
2. **While** not converged ($t<T_{\max}$) **do**
3. Update **Φ** by calling Algorithm 1;
4. Update **Z** by calling Algorithm 2;
5. Compute the objective function value using Eq.(8)
6. $t=t+1$;
7. **Until** Convergence;

Output: $\mathbf{Z}^*$ and $\mathbf{\Phi}^*$;

3.4. Computational Complexity

The Algorithm 3 of DKTL includes two steps: update $\mathbf{\Phi}$ (algorithm 1) and update $\mathbf{Z}$ (algorithm 2). For algorithm 1, the Eigen-decomposition is involved with complexity of $O(N^3)$; for Algorithm 2, the matrix inverse and multiplication are involved with complexity of $O(N^3)$. Therefore, the total complexity of DKTL with T iterations is $O(TN^3)$. It is worth noting that the closed-form solution of $\mathbf{Z}$ can be obtained with $l_{2,1}$-norm, such that the computation of $\mathbf{Z}$ is largely reduced by comparing with that of l_1-norm (*e.g.* ADMM) or *low-rank* (*e.g.* ALM) constraints on $\mathbf{Z}$. Further, the computational time comparison on different tasks is given in Section 5.2.

3.5. Classification

In this paper, we attempt to reduce the domain bias by learning a target data reconstruction model in some latent subspace. The proposed DKTL is independent of classification, and the classification is implemented after solving the optimal $\mathbf{Z}$ and $\mathbf{\Phi}$.

The projected source data in *RKHS* is represented as $\mathbf{K}'_S = \mathbf{\Phi}^{\mathrm{T}}\mathbf{K}_S$ and the reconstructed target data can be represented as $\mathbf{K}'_T = \mathbf{\Phi}^{\mathrm{T}}\mathbf{K}_S\mathbf{Z} \approx \mathbf{\Phi}^{\mathrm{T}}\mathbf{K}_T$. Then, existing classification methods (*e.g.* nearest neighbor, regularized least square, support vector machine) can be used for training a classifier based on the source data $(\mathbf{K}'_S, Y_S)$, and the recognition/test is done on the target data $(\mathbf{K}'_T, Y_T)$. Note that Y_S and Y_T denote the labels with respect to source data and target data, respectively.

4. Experiments

In this section, the experiments on several benchmark datasets, including 3DA object data, 4DA object data, COIL-20 object data, Multi-PIE face data, USPS data, SEMEION data, and MINIST handwritten digits data, have been conducted for evaluating the proposed DKTL method. For classification, the regularized least square classifier and support vector machine can be used.

4.1. Cross-domain Object Recognition

In the experiments of object recognition, we test our method in three domain adaptation benchmark datasets: 3DA office dataset, 4DA office dataset, and COIL-20 object dataset.

3DA data: *Amazon*, *DSLR* and *Webcam* [33].

Table 1

Classification Accuracy (%) over 31 Object Categories of Single Source Domain Adaptation in 3DA Data

Tasks	ASVM [40]	GFK [12]	SGF [13]	RDALR [18]	SA [9]	LTSL [34]	DKTL
Amazon → Webcam	42.2±0.9	46.4±0.5	45.1±0.6	50.7±0.8	48.4±0.6	**53.5**±0.4	53.0±0.8
DSLR → Webcam	33.0±0.8	61.3±0.4	61.4±0.4	36.9±1.9	61.8±0.9	62.4±0.3	**65.7±0.4**
Webcam → DSLR	26.0±0.7	66.3±0.4	63.4±0.5	32.9±1.2	63.4±0.5	63.9±0.3	**73.3±0.5**

Table 2

Classification Accuracy (%) over 31 Object Categories of Multiple Source Domains Adaptation in 3DA data

Tasks	ASVM [40]	GFK [12]	SGF [13]	RDALR [18]	SA [9]	LTSL [34]	DKTL
Amazon+DSLR→Webcam	30.4±0.6	34.3±0.6	31.0±1.6	36.9±1.1	54.4±0.9	55.3±0.3	60.0±**0.5**
Amazon+Webcam→DSLR	25.3±1.1	52.0±0.8	25.0±0.4	31.2±1.3	37.5±1.0	57.7±0.4	**63.7±0.7**
DSLR+Webcam→Amazon	17.3±0.9	21.7±0.5	15.0±0.4	20.9±0.9	16.5±0.4	20.0±0.2	**22.0±0.4**

It's clear that 3DA dataset includes 4106 samples from three domains, where each domain contains 31 object classes, such as back-pack, keyboard, earphone, etc. By following [33], the 800-bin SURF features are used. 5 random splits of the training data in the source and target domain are implemented and the mean accuracies over 31 categories for a single source domain and multiple source domains adaptation are reported in Table 1 and Table 2, respectively. We compare with six methods, including ASVM [40], GFK [12], SGF [13], SA [9], RDALR [18] and LTSL [34]. From the results, we can observe that LSDT with nonlinear kernel function performs much better results than other methods for single source domain adaptation. For multi-source domain adaptation, DKTL outperforms other methods. Additionally, LTSL outperforms RDALR method to a large extent. Therefore, LTSL is compared in the following experiments.

4DA data: *Amazon*, *DSLR*, *Webcam* and *Caltech* [12].

In 4DA dataset, four domains with 2433 samples are included, where each domain contains 10 common object classes selected from 3DA dataset and an extra Caltech 256 dataset. In experiments, the deep convolutional activation feature (DeCAF) of 4DA data is exploited [3]. The CNN with 5 convolutional layers and 3 fully-connected layers is trained on ImageNet-1000 [19]. For deep feature representation of 4DA, the outputs of the 7th fully-connected layer are used as deep features of the 4DA dataset.

Table 3

Classification Accuracy (%) of Different Domain Adaptation based on CNN Feature in 4DA Setting

Method	A→D	C→D	A→C	W→C	D→C	D→A	W→A	C→A	C→W	A→W
NaïveComb	94.1±0.8	92.8±0.7	83.4±0.4	81.2±0.4	82.7±0.4	90.9±0.3	90.6±0.2	90.3±0.2	90.6±0.8	91.1±0.8
SGF [13]	92.0±1.3	92.4±1.1	77.4±0.7	76.8±0.7	78.2±0.7	88.0±0.5	86.8±0.7	89.3±0.4	87.8±0.8	88.1±0.8
GFK [12]	94.3±0.7	91.9±0.8	79.1±0.7	76.1±0.7	77.5±0.8	90.1±0.4	85.6±0.5	88.4±0.4	86.4±0.7	88.6±0.8
SA [9]	92.8±1.0	92.1±0.9	83.3±0.2	81.0±0.6	82.9±0.7	90.7±0.5	90.9±0.4	89.9±0.5	89.0±1.1	87.8±1.4
LTSL [34]	94.5±0.5	93.5±0.8	85.4±0.1	82.6±0.3	84.8±0.2	91.9±0.2	91.0±0.2	90.9±0.1	90.8±0.7	91.5±0.5
DKTL	**96.6±0.5**	**94.3±0.6**	**86.7±0.3**	**84.0±0.3**	**86.1±0.4**	**92.5±0.3**	**91.9±0.3**	**92.4±0.1**	**92.0±0.9**	**93.0±0.8**

Table 4

Comparisons with deep transfer learning methods on 4DA dataset

Method	A→D	C→D	A→C	W→C	D→C	D→A	W→A	C→A	C→W	A→W	Average
AlexNet [19]	88.3	87.3	77.9	77.9	81.0	89.0	83.1	91.3	83.2	83.1	84.2
DDC [38]	89.0	88.8	85.0	78.0	81.1	89.5	84.9	91.9	85.4	86.1	86.0
DAN [28]	92.4	90.5	85.1	84.3	82.4	92.0	92.1	92.0	90.6	93.8	89.5
RTN [27]	94.6	92.9	88.5	**88.4**	84.3	**95.5**	**93.1**	**94.4**	**96.6**	**97.0**	**92.5**
DKTL	**96.6**	**94.3**	**86.7**	84.0	**86.1**	92.5	91.9	92.4	92.0	93.0	91.0

We strictly follow the experimental setting by Gong *et al.*[12], 20 random splits of the training data are used, and the mean classification accuracies on CNN deep features are reported in Table 3. By comparing to state-of-the-art methods, from Table 3, we can clearly observe that DKTL performs much better than LTSL and also outperforms other methods. Further, we have also compared with several deep transfer learning methods, such as AlexNet [19], deep domain confusion (DDC) [38], deep adaptation network (DAN) [28], and residual transfer network (RTN) [27] on the 4DA dataset. The comparisons are shown in Table 4. Notably, for our method, the off-the-shelf CNN based DeCAF feature is used for fair comparison. Due to that the repetitive running experiments of these deep transfer models are not easy, for better subjectivity, the results in Table 4 of deep transfer learning methods are copied from the RTN paper [27]. From Table 4, we can see that although the RTN shows better performance than DKTL, our method still shows competitive performance among deep transfer models. Specifically, the average result of DKTL is 91%, which is 1.5% lower than RTN, but 1.5% higher than DAN, and 6.8% higher than AlexNet. Additionally, the visualization of the representation based transfer coefficients **Z** can be observed in Fig. 3.

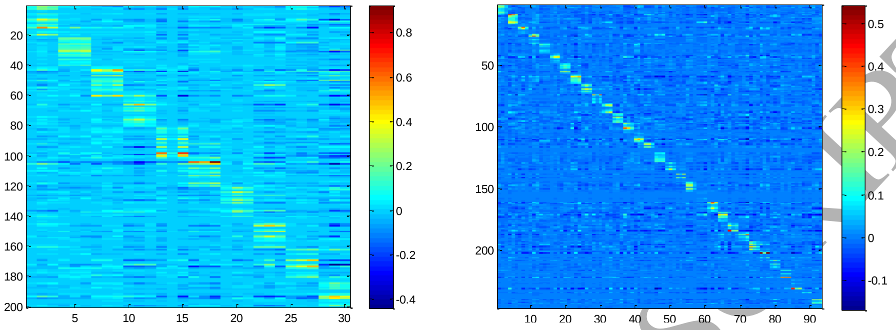

(a) **Z** on 4DA data

(b) **Z** on 3DA data

Fig. 3. Visualization of the solved representation coefficients **Z**

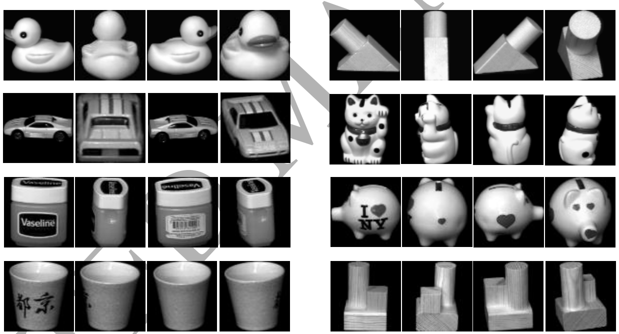

Fig. 4. Several objects from COIL-20 data (e.g. COIL 1, 2, 3, and 4)

COIL-20 data: *Columbia Object Image Library* [30].

The domain adaptation experiment on COIL-20 dataset was first announced by Long *et al.* [25]. The COIL-20 dataset contains 1440 gray scale images of 20 objects (72 images with different poses per object). The objects have a wide variety of complex geometric and reflectance characteristics, and can effectively validate the cross domain learning models. Each image has 128×128 pixels with 256 gray levels per pixel. For experiments, the size of each image is adjusted as 32×32 [39]. Some example images of this dataset are shown in Fig. 4.

Table 5

Classification Accuracy (%) On Coil-20 Dataset

Source	Target	ASVM [40]	GFK [12]	SGF [13]	SA [9]	LTSL [34]	DKTL
COIL 1	COIL 2	79.7	81.1	78.9	81.1	79.7	83.8
COIL 1	COIL 3	76.8	80.1	76.7	75.3	79.2	79.7
COIL 1	COIL 4	81.4	80.0	74.7	76.7	81.4	80.0
COIL 2	COIL 1	78.3	80.0	79.2	81.1	76.4	81.1
COIL 2	COIL 3	84.3	85.0	79.7	81.9	86.4	85.6
COIL 2	COIL 4	77.2	78.9	74.4	78.3	77.2	79.7
COIL 3	COIL 1	76.4	79.7	71.1	78.9	76.4	80.8
COIL 3	COIL 2	79.6	83.0	81.1	80.3	79.7	82.8
COIL 3	COIL 4	74.2	73.3	73.3	76.1	74.2	75.8
COIL 4	COIL 1	81.9	81.1	72.5	79.4	81.9	81.7
COIL 4	COIL 2	77.5	79.2	71.1	72.8	77.8	78.6
COIL 4	COIL 3	74.8	75.6	76.7	78.3	74.7	79.2
Average		78.5	79.7	75.8	78.4	78.8	**80.7**

In experimental setup, the dataset is partitioned into four subsets, i.e. COIL 1, COIL 2, COIL 3 and COIL 4 according to the directions as shown in Fig. 4. Specifically, COIL 1 contains all images captured with the angle of [0º, 85º], such that the number of all images is 360. COIL 2 are with the angle of [180º, 265º], and the number of all images is 360. COIL 3 contains all images captured with the angle of [90º, 175º] with 360 images, and COIL 4 are captured in the angle of [270º, 355º], and the number of all images is 360. For validating the proposed cross domain learning method, 12 pairwise settings of four different domains are used for constructing the heterogeneous source and target data.

Setting 1: COIL 1 (source domain) and COIL 2 (target domain), i.e. COIL 1→COIL 2.

Setting 2: COIL 1 (source domain) and COIL 3 (target domain), i.e. COIL 1→COIL 3.

…

Setting 12: COIL 4 (source domain) and COIL 3 (target domain), i.e. COIL 4→COIL 3.

The experimental results for 12 settings are reported in Table 5, from which we can observe that the proposed DKTL method achieves the best performance with an average recognition accuracy of 80.7%.

Fig. 5. CMU Multi-PIE data. Session 1 (the 1st row with neutral expression) and Session 2 (the 2nd row with smile expression)

4.2. Cross-poses Face Recognition

The CMU Multi-PIE face dataset [15] is a comprehensive face dataset of 337 subjects, in which the images are captured across 15 poses, 20 illuminations, 6 expressions and 4 different sessions. For our purpose, we select the first 60 subjects from session 1 and session 2 in experiments. Session 1 contains 7 images per subject with 7 poses under neutral expression, while session 2 was prepared with the same poses as session 1 under smile expression. Similar domain adaptation experiment on PIE has been first conducted by Long *et al.* [25]. In this paper, four cross-domain recognition tasks are as follows.

- ✧ Session 1 (cross-poses): one frontal face and an extreme pose with 60° angle for each subject are used as source and target data, respectively. The remaining faces are used as probe faces.
- ✧ Session 2 (cross-poses): the same configuration as session 1 is conducted on session 2.
- ✧ Session 1+2 (cross-poses): Two frontal faces and two faces with extreme 60° pose from both sessions are selected as source and target data. The remaining faces with poses are used as probe faces.
- ✧ Cross session: The faces in session 1 with neural expression are taken as source data, while the faces in session 2 with smile expression are taken as target data.

Fig. 5 describes some examples of one subject which consists of two sessions (neutral vs. smile expressions). From Fig. 5, we can observe the highly nonlinear domain mismatch between frontal faces and posed faces, while the domain mismatch between neutral and smile faces of the same view is slightly insignificant.

The face recognition results by using different methods are shown in Table 6. From the results, we can see that the proposed DKTL method outperforms LTSL and others. This demonstrates that linear subspace transfer may not deal with such nonlinear rotation well. For cross-session task, the recognition gap is small due to that expression change is much easier to be adapted than pose.

Table 6

Comparison with Other Methods for Face Recognition Across Poses and Expression

Cross domain tasks	NaïveComb	ASVM [40]	SGF [13]	GFK [12]	SA [9]	LTSL [34]	DKTL
Session 1: Frontal → 60° pose	52.0	52.0	53.7	56.0	51.3	61.0	**66.0**
Session 2: Frontal → 60° pose	55.0	56.7	55.0	58.7	62.7	62.7	**71.0**
Session 1+2: Frontal → 60° pose	54.5	55.1	53.8	56.3	61.7	60.2	**69.5**
Cross session: Session 1 → Session 2	93.6	97.2	92.5	96.7	98.3	97.2	**99.4**

Fig. 6. Handwritten digits (0~9) from different sources: SEMEION (1st row), USPS (2nd row) and MINIST (3rd row)

4.3. Cross-domain Handwritten Digits Recognition

The domain adaptation experiment on handwritten digit recognition was first proposed by Long *et al.* [26]. In this paper, three handwritten digits datasets, MINIST [21], USPS [10] and SEMEION [10] are used for evaluating the proposed cross domain learning method. The classification accuracies over 10 classes from digit 0~9 are reported for different tasks. The MINIST handwritten digits dataset consists of 70,000 instances with each image size of 28×28, the USPS dataset contains 9298 examples with each image size of 16×16, and the SEMEION dataset contains 2593 images with each image size of 16×16.

For dimension consistency, the size of MINIST digit images is manually cropped as 16×16. The example images of each class in MINIST, USPS and SEMEION are shown in Fig. 6, from which we can clearly observe the significant domain mismatch across different domains.

In experiment, the cross-domain tests are explored, in which each dataset is viewed as one domain, and therefore formulates 6 cross-domain tasks in pairwise. For the purpose of our experiments, we randomly select 100 samples per class from a source domain for training and 10 samples per class from the target domain for testing. In this way, 5 random splits are generated and the mean accuracies with parameter tuning are reported in Table 7, in which A-SVM [40], SGF [13], GFK [12] and LTSL [34] are compared with our proposed DKTL method. From the results, we can see that the proposed method outperforms other methods to a large extent.

Table 7

Handwritten Digits Recognition Performance Across Different Domains

Source	Target	NaïveComb	A-SVM [40]	SGF [13]	GFK [12]	SA [9]	LTSL [34]	DKTL
MINIST	USPS	78.8±0.5	78.3±0.6	79.2±0.9	82.6±0.8	78.8±0.8	78.4±0.7	**88.0±0.4**
SEMEION	USPS	83.6±0.3	76.8±0.4	77.5±0.9	82.7±0.6	82.5±0.5	83.4±0.3	**85.8±0.4**
MINIST	SEMEION	51.9±0.8	70.5±0.7	51.6±0.7	70.5±0.8	74.4±0.6	50.6±0.4	**74.9±0.4**
USPS	SEMEION	65.3±1.0	74.5±0.6	70.9±0.8	76.7±0.3	74.6±0.6	64.5±0.7	**81.6±0.4**
USPS	MINIST	71.7±1.0	73.2±0.8	71.1±0.7	74.9±0.9	72.9±0.7	71.2±1.0	**79.0±0.6**
SEMEION	MINIST	67.6±1.2	69.3±0.7	66.9±0.6	74.5±0.6	72.9±0.7	66.8±1.2	**77.3±0.7**

4.4. Discussion

With the above experiments on several benchmark datasets, we can observe the competitive effectiveness of the proposed DKTL method via $l_{2,1}$-norm minimization. The proposed joint *domain-class-consistency* realized using a kernel sparse representation and discriminative cross-domain subspace learning shows a new perspective and interest of transfer learning. Specifically, the following insights are observed.

1) The shadow of kernel learning, discriminative learning, subspace learning and representation learning can be witnessed in the proposed method for transfer learning tasks. It implies that a number of statistical machine learning methods can be well "fitted" to multi-domain tasks with appropriate transferring.

2) The fundamental problem that transfer learning aims to solve is to overcome the statistical distribution mismatch induced cross-domain classification (e.g. source domain vs. target domain). How to quantify the distribution mismatch metric is the basic motivation of this proposal. Robust reconstruction and calibration between domains in some latent subspace is the main line of this paper, while a specifically designed reconstruction error, as domain mismatch, is minimized.

3) Nonlinear transfer is a common problem in computer vision, and therefore kernel space mapping is extremely appropriate to deal with such problems. Additionally, transferring should be conducted in a latent

subspace, so that the testing phase can be effectively manifested based on this subspace projection.

5. Parameter Sensitivity and Computational Time Analysis

5.1. Parameter sensitivity analysis

In the proposed DKTL model, there are two hyper-parameters λ and τ. Additionally, there are also several internal model parameters such as the dimensionality d, the kernel parameter σ, and the constrained coefficient α_S. For more insight of their impact on the model, we have provided parameter sensitivity analysis in this section. Specifically, the hyper-parameters λ and τ are tuned in the range of 10^{-4}~10^{4}, the kernel parameter σ is tuned in the range of 2^{-4}~2^{4}, and the coefficient α_S is tuned in the range of 0~1. The optimal dimensionality d is task-specific, therefore it is empirically tuned from low to high.

For better insight of the parameter sensitivity, we have conducted experiments on Multi-PIE dataset (Cross session: Session 1 → Session 2) and Handwritten digit dataset (MINIST → USPS). The parameter sensitivity analysis is described in Fig.7, in which Fig.7(a) denotes the results of face recognition and Fig.7(b) represents the handwritten digit recognition results. From Fig. 7, we observe that the optimal parameter tuning can be easily determined for different cross-domain tasks.

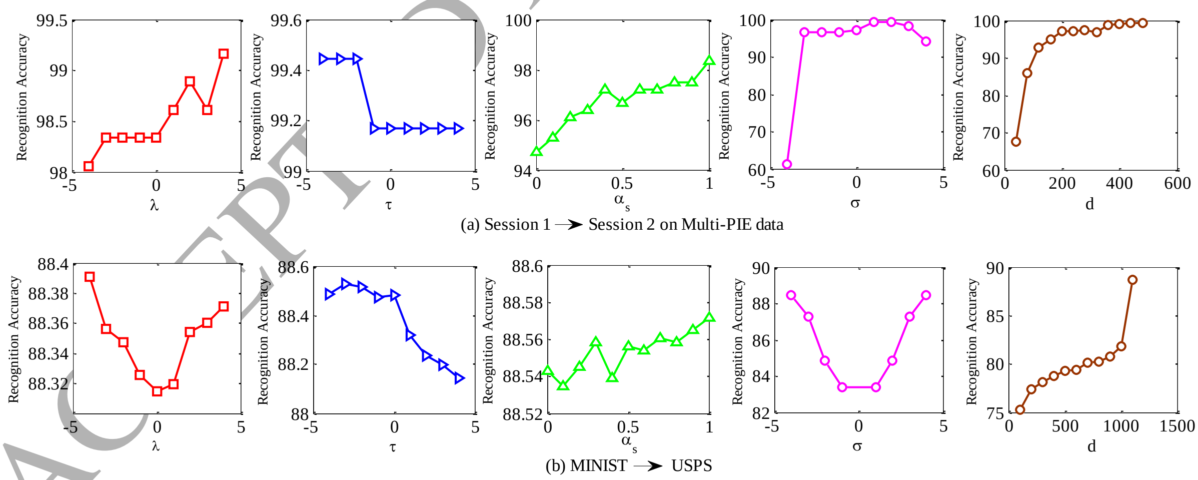

Fig. 7. Parameter sensitivity analysis on (a) face recognition task and (b) handwritten digit recognition task

5.2. Computational time analysis

In this section, the computational time analysis is empirically provided for comparing with other algorithms. Specifically, we have compared with SGF [13], GFK [12], SA [9], and LTSL [34] methods on two tasks: face recognition and handwritten digits recognition. The computational time is shown in Table 8, where the numbers in brackets represent the recognition accuracy of each method. From Table 8, we observe that the proposed method is slightly slower than other methods, due to the kernel computation in DKTL. However, the domain transfer performance of the proposed method is higher than other methods. Therefore, with the trade-off between computation and performance, the proposed DKTL still shows more competitive results.

Table 8

Empirical computational time (s) analysis of different methods

Source	Target	SGF [13]	GFK [12]	SA [9]	LTSL [34]	DKTL
PIE Session 1	PIE Session 2	10.9 (92.5%)	1.50 (96.7%)	4.18 (98.3%)	7.21 (97.2%)	7.48 (99.4%)
MINIST	USPS	75.0 (79.2%)	12.2 (82.6%)	30.5 (78.8%)	62.1 (78.4%)	96.9 (88.0%)

6. Conclusion

In this paper, we propose a discriminative kernel transfer learning (DKTL) via $l_{2,1}$-norm minimization. In the model, the domain class consistency (DCC) that simultaneously interprets the domain consistency and class consistency (double consistency) is proposed. To this end, in subspace learning, the discriminative mechanism for strengthening the importance of between-domain intra-class consistency and within-domain inter-class inconsistency is integrated. For reducing the domain inconsistency, we tend to learn a representation coefficient matrix between the source data and the target data in the learned discriminative subspace. To avoid the potential outliers in source domain transferred to the target domain after representation, the $l_{2,1}$-norm constraint is imposed, such that a few valuable source data points are selected during representation based transfer learning. Extensive experiments on several benchmark datasets demonstrate that the effectiveness, superiority and competitiveness of the proposed DKTL method.

Appendix A

Deduction of Eq.(11) derivation

The Eq. (10) can be re-written as

$$\min_{\boldsymbol{\Phi}} Tr\left(\boldsymbol{\Phi}^{\mathrm{T}}\mathbf{K}_T - \boldsymbol{\Phi}^{\mathrm{T}}\mathbf{K}_S\mathbf{Z}\right)\left(\boldsymbol{\Phi}^{\mathrm{T}}\mathbf{K}_T - \boldsymbol{\Phi}^{\mathrm{T}}\mathbf{K}_S\mathbf{Z}\right)^{\mathrm{T}} + \lambda\cdot\left(Tr\left(\frac{1}{C}\cdot\sum_{c=1}^{C}\left(\boldsymbol{\Phi}^{\mathrm{T}}\mathbf{K}_{\mu,S}^{c} - \boldsymbol{\Phi}^{\mathrm{T}}\mathbf{K}_{\mu,T}^{c}\right)\left(\boldsymbol{\Phi}^{\mathrm{T}}\mathbf{K}_{\mu,S}^{c} - \boldsymbol{\Phi}^{\mathrm{T}}\mathbf{K}_{\mu,T}^{c}\right)^{\mathrm{T}}\right)\right.$$

$$\left.- Tr\left(\frac{2}{C(C-1)}\sum_{t\in\{S,T\}}\alpha_t\cdot\sum_{c,k=1,c\neq k}^{C}\left(\boldsymbol{\Phi}^{\mathrm{T}}\mathbf{K}_{\mu,t}^{c} - \boldsymbol{\Phi}^{\mathrm{T}}\mathbf{K}_{\mu,t}^{k}\right)\left(\boldsymbol{\Phi}^{\mathrm{T}}\mathbf{K}_{\mu,t}^{c} - \boldsymbol{\Phi}^{\mathrm{T}}\mathbf{K}_{\mu,t}^{k}\right)^{\mathrm{T}}\right)\right)$$

$$s.t.\ \boldsymbol{\Phi}^{\mathrm{T}}\mathbf{K}\boldsymbol{\Phi} = \mathbf{I},\ \alpha_S + \alpha_T = 1,\ \lambda, \alpha_S, \alpha_T > 0$$

$$\Rightarrow \min_{\boldsymbol{\Phi}} Tr\left(\boldsymbol{\Phi}^{\mathrm{T}}\left(\mathbf{K}_T - \mathbf{K}_S\mathbf{Z}\right)\left(\mathbf{K}_T - \mathbf{K}_S\mathbf{Z}\right)^{\mathrm{T}}\boldsymbol{\Phi}\right) + \lambda\cdot\left(Tr\left(\boldsymbol{\Phi}^{\mathrm{T}}\frac{1}{C}\cdot\sum_{c=1}^{C}\left(\mathbf{K}_{\mu,S}^{c} - \mathbf{K}_{\mu,T}^{c}\right)\left(\mathbf{K}_{\mu,S}^{c} - \mathbf{K}_{\mu,T}^{c}\right)^{\mathrm{T}}\boldsymbol{\Phi}\right) - \right.$$

$$\left. Tr\left(\boldsymbol{\Phi}^{\mathrm{T}}\frac{2}{C(C-1)}\sum_{t\in\{S,T\}}\alpha_t\cdot\sum_{c,k=1,c\neq k}^{C}\left(\mathbf{K}_{\mu,t}^{c} - \mathbf{K}_{\mu,t}^{k}\right)\left(\mathbf{K}_{\mu,t}^{c} - \mathbf{K}_{\mu,t}^{k}\right)^{\mathrm{T}}\boldsymbol{\Phi}\right)\right)$$

$$s.t.\ \boldsymbol{\Phi}^{\mathrm{T}}\mathbf{K}\boldsymbol{\Phi} = \mathbf{I},\ \alpha_S + \alpha_T = 1,\ \lambda, \alpha_S, \alpha_T > 0$$

$$\Rightarrow \min_{\boldsymbol{\Phi}} Tr\left(\boldsymbol{\Phi}^{\mathrm{T}}\mathbf{A}_1\boldsymbol{\Phi}\right) + \lambda\cdot\left(Tr\left(\boldsymbol{\Phi}^{\mathrm{T}}\mathbf{A}_2\boldsymbol{\Phi}\right) - Tr\left(\boldsymbol{\Phi}^{\mathrm{T}}\mathbf{A}_3\boldsymbol{\Phi}\right)\right)$$

$$s.t.\ \boldsymbol{\Phi}^{\mathrm{T}}\mathbf{K}\boldsymbol{\Phi} = \mathbf{I},\ \alpha_S + \alpha_T = 1,\ \lambda, \alpha_S, \alpha_T > 0$$

$$\Rightarrow \min_{\boldsymbol{\Phi}} Tr\left(\boldsymbol{\Phi}^{\mathrm{T}}\left(\mathbf{A}_1 + \lambda\cdot\mathbf{A}_2 - \lambda\cdot\mathbf{A}_3\right)\boldsymbol{\Phi}\right)$$

$$= \min_{\boldsymbol{\Phi}} Tr\left(\boldsymbol{\Phi}^{\mathrm{T}}\mathbf{A}\boldsymbol{\Phi}\right)$$

$$s.t.\ \boldsymbol{\Phi}^{\mathrm{T}}\mathbf{K}\boldsymbol{\Phi} = \mathbf{I},\ \alpha_S + \alpha_T = 1,\ \lambda, \alpha_S, \alpha_T > 0$$

where $\mathbf{A}$, $\mathbf{A}_1$, $\mathbf{A}_2$, $\mathbf{A}_3$ are represented in Eqs.(12), (13), (14) and (15), respectively.

Appendix B

Optimization of model Eq.(11)

According to Eq.(11), the Lagrange multiplier function $Lag(\cdot)$ can be expressed as

$$Lag(\boldsymbol{\Phi}, \rho) = \boldsymbol{\Phi}^{\mathrm{T}}\mathbf{A}\boldsymbol{\Phi} - \rho\cdot\left(\boldsymbol{\Phi}^{\mathrm{T}}\mathbf{K}\boldsymbol{\Phi} - \mathbf{I}\right) \tag{22}$$

where $\rho>0$ represents the Lagrange multiplier.

By setting the derivative of Eq.(22) with respect to $\boldsymbol{\Phi}$ as 0, one can obtain

$$\mathbf{A}\boldsymbol{\Phi} = \rho\cdot\mathbf{K}\boldsymbol{\Phi} \rightarrow \mathbf{K}^{-1}\mathbf{A}\boldsymbol{\Phi} = \rho\cdot\boldsymbol{\Phi} \tag{23}$$

From Eq.(23), we can get that $\mathbf{\Phi}$ can be solved by using the following Eigen-value decomposition

$$\mathbf{K}^{-1}\mathbf{A} = \mathbf{U}\Sigma\mathbf{U}^{\mathrm{T}} \tag{24}$$

Then, $\mathbf{\Phi}$ is represented by the first l Eigen-vectors in $\mathbf{U}$, with respect to the first l minimum Eigen-values of the matrix Σ .

Acknowledgment

The authors would like to thank the AE and anonymous reviewers for their insightful and constructive comments. This work was supported by the Fundamental Research Funds for the Central Universities (Project No. 106112017CDJQJ168819), the National Natural Science Foundation of China under Grants 61401048, 91420201 and 61472187, the 973 Program No.2014CB349303, and Program for Changjiang Scholars.

References

[1] R. Collobert, F. Sinz, J. Weston, and L. Bottou, Large scale transductive SVMs, *Journal of Machine Learning Research*, 7 (2006) 1687-1712.

[2] H. Daumé. Frustratingly easy domain adaptation, *ACL*, 45: 256-263, 2007.

[3] J. Donahue, Y. Jia, O. Vinyals, J. Hoffman, N. Zhang, E. Tzeng, T. Darrell, DeCAF: A Deep Convolutional Activation Feature for Generic Visual Recognition, *ICML*, 2014.

[4] L. Duan, W. Tsang, and D. Xu. Domain Transfer Multiple Kernel Learning, *IEEE Trans. Pattern Anal. Mach. Intell*. 34(3) (2012) 465-479.

[5] L. Duan, D. Xu, and I. Tsang, Domain adaptation from multiple sources: A domain-dependent regularization approach, *IEEE Trans. Neural Networks and Learning Systems*, 23 (3) (2012) 504-518.

[6] L. Duan, D. Xu, W. Tsang, and J. Luo. Visual Event Recognition in Videos by Learning from Web Data. *IEEE Trans. Pattern Anal. Mach. Intell*. 34 (9) (2012) 1667-1680.

[7] E. Elhamifar and R. Vidal. Sparse subspace clustering. *CVPR*, 2009, pp. 2790-2797.

[8] E. Elhamifar and R. Vidal. Sparse subspace clustering: Algorithm, theory, and applications. *IEEE Trans. Pattern Anal. Mach. Intell.* 35 (11) (2013) 2675-2781.

[9] B. Fernando, A. Habrard, M. Sebban, and T. Tuytelaars, Unsupervised Visual Domain Adaptation Using Subspace Alignment, *ICCV,* 2013, pp. 2960-2967.

[10] A. Frank and A. Asuncion, (2010) UCI machine learning repository [Online]. Available: http://archive.ics.uci.edu/ml

[11] Y. Ganin and V.S. Lempitsky, Unsupervised Domain Adaptation by Backpropagation, *ICML*, 2015, 1180-1189.

[12] B. Gong, Y. Shi, F. Sha, and K. Grauman. Geodesic flow kernel for unsupervised domain adaptation, *CVPR*, 2012, 2066-2073.

[13] R. Gopalan, R. Li, and R. Chellappa. Domain adaptation for object recognition: An unsupervised approach, *ICCV*, 2011.

[14] G. Griffin, A. Holub, and P. Perona. Caltech-256 object category dataset, Tech.rep. 2007.

[15] R. Gross, I. Matthews, J.F. Cohn, T. Kanade, and S. Baker. Multi-pie. *Image Vision Computing*, 28 (5) (2010) 807-813.

[16] J. Hoffman, E. Rodner, J. Donahue, B. Kulis, K. Saenko. Asymmetric and Category Invariant Feature Transformations for Domain Adaptation, *Int. J. Comput. Vis.* 109 (2014) 28-41.

[17] C. Hou, F. Nie, X. Li, D. Yi, and Y. Wu, Joint Embedding Learning and Sparse Regression: A Framework for Unsupervised Feature Selection, *IEEE Trans. Cybernetics*, 44 (6) (2014) 793-804.

[18] I.H. Jhuo, D. Liu, D. Lee, and S.F. Chang. Robust visual domain adaptation with low-rank reconstruction, *CVPR*, 2012, pp. 2168-2175.

[19] A. Krizhevsky, I. Sutskever, G.E. Hinton, ImageNet classification with deep convolutional neural networks, *NIPS*, 2012.

[20] B. Kulis, K. Saenko, and T. Darrell. What you saw is not what you get: Domain adaptation using asymmetric kernel transforms, *CVPR*, 2011, 20-25.

[21] Y. LeCun, L. Bottou, Y. Bengio, and P. Haffner, "Gradient-based learning applied to document recognition," *Proceedings of the IEEE*, 86 (11) (1998) 2278-2324.

[22] G. Liu, Z. Lin, and Y. Yu. Robust subspace segmentation by low-rank representation. *ICML*, 2010, pp.663-670.

[23] G. Liu, Z. Lin, S. Yan, J. Sun, Y. Yu, and Y. Ma. Robust recovery of subspace structures by low-rank representation. *IEEE Trans. Pattern Anal. Mach. Intell.* 35(1) (2013) 171-184.

[24] M. Long, J. Wang, G. Ding, S.J. Pan, and P.S. Yu, Adaptation Regularization: A General Framework for Transfer Learning, *IEEE Trans. Knowledge and Data Engineering*, 26 (5) 1076-1089, 2014.

[25] M. Long, J. Wang, G. Ding, J. Sun, and P.S. Yu, Transfer Feature Learning with Joint Distribution Adaptation, *ICCV*, 2013, pp. 2200-2207.

[26] M. Long, J. Wang, G. Ding, J. Sun, and P.S. Yu, Transfer Joint Matching for Unsupervised Domain Adaptation, *CVPR*, 2014, pp. 1410-1417.

[27] M. Long, H. Zhu, J. Wang, and M.I. Jordan, Unsupervised Domain Adaptation with Residual Transfer Networks, *NIPS*, 2016.

[28] M. Long, Y. Cao, J. Wang, M.I. Jordan, Learning Transferable Features with Deep Adaptation Networks, *ICML*, 2015, 97-105.

[29] M. Long, J. Wang, Y. Cao, J. Sun, and P.S. Yu, "Deep Learning of Transferable Representation for Scalable Domain Adaptation," *IEEE Trans. Knowledge and Data Engineering*, 28 (8) 2027-2040, 2016.

[30] S.A. Nene, S.K. Nayar, and H. Murase, Columbia Object Image Library (COIL-20), Tech. Rep., No. CUCS-006-96.

[31] F. Nie, H. Huang, X. Cai, and C. Ding, Efficient and Robust Feature Selection via Joint $l_{2,1}$-Norm Minimization, *NIPS*, 2010.

[32] S.J. Pan, Q. Yang, A survey on transfer learning, *IEEE Trans. Knowl. Data Eng.*, 2010.

[33] K. Saenko, B. Kulis, M. Fritz, and T. Darrell. Adapting visual category models to new Domains, *ECCV*, 2010.

[34] M. Shao, D. Kit, and Y. Fu. Generalized Transfer Subspace Learning Through Low-Rank Constraint, *Int. J. Comput. Vis.*, 109 (2014) 74-93.

[35] L. Shao, F. Zhu, and X. Li, Transfer Learning for Visual Categorization: A Survey, IEEE Trans. Neural Networks and Learning

Systems, vol. 26, no. 5, 1019-1034, 2015.

[36] S. Shekhar, V.M. Patel, H.V. Nguyen, and R. Chellappa. Generalized Domain-Adaptive Dictionaries, *CVPR*, 2013, 361-368.

[37] E. Tzeng, J. Hoffman, T. Darrell, and K. Saenko, "Simultaneous Deep Transfer Across Domains and Tasks," *ICCV*, 2015, pp. 4068-4076.

[38] E. Tzeng, J. Hoffman, N. Zhang, K. Saenko, and T. Darrell, "Deep domain confusion: Maximizing for domain invariance," arXiv, 2014.

[39] Y. Xu, X. Fang, J. Wu, X. Li, and D. Zhang, Discriminative Transfer Subspace Learning via Low-Rank and Sparse Representation, *IEEE Transactions on Image Processing*, 25 (2) (2016) 850-863.

[40] J. Yang, R. Yan, and A. Hauptmann. Cross-domain video concept detection using adaptive SVMs, *ACM MM*. 2007.

[41] L. Zhang and D. Zhang, MetricFusion: Generalized Metric Swarm Learning for Similarity Measure, Information Fusion 30 (2016) 80-90.

[42] L. Zhang and D. Zhang, Domain Adaptation Extreme Learning Machines for Drift Compensation in E-nose Systems, *IEEE Trans. Instru. Meas.* 64 (7) (2015) 1790-1801.

[43] L. Zhang, W. Zuo and D. Zhang, LSDT: Latent Sparse Domain Transfer Learning for Visual Adaptation, *IEEE Trans. Image Processing*, 25 (3) (2016) 1177-1191.

[44] L. Zhang, Y. Liu, and P. Deng, Odor Recognition in Multiple E-nose Systems with Cross-domain Discriminative Subspace Learning, *IEEE Trans. Instrumentation and Measurement*, 2017. In press.

[45] L. Zhang, S.K. Jha, T. Liu, and G. Pei, Discriminative Kernel Transfer Learning via $l_{2,1}$-Norm Minimization, *IJCNN*, 2016, 2220-2227.

[46] L. Zhang and D. Zhang, Robust Visual Knowledge Transfer via Extreme Learning Machine based Domain Adaptation, *IEEE Trans. Image Processing*, 25 (10) 4959-4973, 2016.

[47] F. Zheng, Y. Tang, and L. Shao, Hetero-manifold Regularization for Cross-modal Hashing, *IEEE Trans. Pattern Analysis and Machine Intelligence*, 2016. In press.

[48] F. Zhu and L. Shao, Weakly-Supervised Cross-Domain Dictionary Learning for Visual Recognition, *International Journal of Computer Vision*, 109 (1) (2014) 42-59.

[49] F. Zhu, L. Shao, and Y. Fang, Boosted Cross-Domain Dictionary Learning for Visual Categorization, *IEEE Intelligent Systems*, 31 (3) 6-18, 2016.

Biographies

Lei Zhang received his Ph.D degree in Circuits and Systems from the College of Communication Engineering, Chongqing University, Chongqing, China, in 2013. He is currently a Professor/Distinguished Research Fellow with Chongqing University. He was selected as a Hong Kong Scholar in China in 2013, and worked as a Post-Doctoral Fellow with The Hong Kong Polytechnic University, Hong Kong, from 2013 to 2015. He has authored more than 60 scientific papers in top journals, including the IEEE Transactions, such as T-NNLS, T-IP, T-MM, T-SMCA, T-IM, IEEE Sensors Journal, Information Fusion, Sensors & Actuators B, Neurocomputing, and Analytica Chimica Acta, etc. His current research interests include machine learning, pattern recognition, computer vision and intelligent system. Dr. Zhang was a recipient of Outstanding Doctoral Dissertation Award of Chongqing, China, in 2015, Hong Kong Scholar Award in 2014, Academy Award for Youth Innovation of Chongqing University in 2013 and the New Academic Researcher Award for Doctoral Candidates from the Ministry of Education, China, in 2012.

Jian Yang received the PhD degree from Nanjing University of Science and Technology (NUST), on the subject of pattern recognition and intelligence systems in 2002. In 2003, he was a postdoctoral researcher at the University of Zaragoza. From 2004 to 2006, he was a Postdoctoral Fellow at Biometrics Centre of Hong Kong Polytechnic University. From 2006 to 2007, he was a Postdoctoral Fellow at Department of Computer Science of New Jersey Institute of Technology. Now, he is a Chang-Jiang professor in the School of Computer Science and Technology of NUST. He is the author of more than 100 scientific papers in pattern recognition and computer vision. His journal papers have been cited more than 4000 times in the ISI Web of Science, and 9000 times in the Web of Scholar Google. His research interests include pattern recognition, computer vision and machine learning. Currently, he is/was an associate editor of Pattern Recognition Letters, IEEE Trans. Neural Networks and Learning Systems, and Neurocomputing. He is a Fellow of IAPR.

David Zhang graduated in Computer Science from Peking University. He received his MSc in 1982 and his PhD in 1985 in Computer Science from the Harbin Institute of Technology (HIT), respectively. From 1986 to 1988 he was a Postdoctoral Fellow at Tsinghua University and then an Associate Professor at the Academia Sinica, Beijing. In 1994 he received his second PhD in Electrical and Computer Engineering from the University of Waterloo, Ontario, Canada. He is a Chair Professor since 2005 at the Hong Kong Polytechnic University where he is the Founding Director of the Biometrics Research Centre (UGC/CRC) supported by the Hong Kong SAR Government in 1998. He also serves as Visiting Chair Professor in Tsinghua University, and Adjunct Professor in Peking University, Shanghai Jiao Tong University, HIT, and the University of Waterloo. He is the Founder and Editor-in-Chief, International Journal of Image and Graphics (IJIG); Book Editor, Springer International Series on Biometrics (KISB); Organizer, the International Conference on Biometrics Authentication (ICBA); Associate Editor of more than ten international journals including IEEE Transactions and so on; and the author of more than **10** books, over **300** international journal papers and **30** patents from USA/Japan/HK/China. Professor Zhang is a Croucher Senior Research Fellow, Distinguished Speaker of the IEEE Computer Society, and a Fellow of both IEEE and IAPR.